International Conference on Mathematics, Computational Methods & Reactor Physics (M&C 2009)
Saratoga Springs, New York, May 3-7, 2009, on CD-ROM, American Nuclear Society, LaGrange Park, IL (2009)

A CONSISTENT DIFFUSION SYNTHETIC ACCELERATION TECHNIQUE UTILISING DISCONTINUITY FACTORS

Alan Copestake
Rolls-Royce plc
PO Box 2000
Derby
DE21 7XX
UK
alan.copestake@rolls-royce.com

ABSTRACT

This paper describes a consistent Diffusion Synthetic Acceleration (DSA) technique that utilises Discontinuity Factors to correctly calculate interfacial currents via Equivalence Theory. This equivalence DSA (eDSA) is used to accelerate the solution of the finite difference S_N discrete ordinates Boltzmann transport equation in regular Cartesian geometry. The paper describes how this eDSA technique can be applied to accelerate both the inner (transport sweep) and, most favorably, the outer (scatter and fission source) iteration process. The application of the method is illustrated by reference to the OECD NEA C5G7 2D benchmark problem. It is shown that the method will reduce the number of fission source iterations required by at least a factor of ten, and that, with the use of this technique, the computational cost of higher order discrete ordinates solutions rises at less than order N. Finally, suggestions are made as to how the method might be applied to other transport theory solution techniques.

Key Words: DSA, Equivalence Theory, Discontinuity Factor, Acceleration.

1. INTRODUCTION

The Diffusion Synthetic Acceleration (DSA) technique [1] is a well known and efficient method of accelerating the solution of the discrete ordinates Boltzmann transport equation. This technique, however, suffers from inconsistencies in the definition of the diffusion coefficient such that the diffusion theory approximation does not correctly reproduce the transport theory interfacial currents, leading to problems with convergence in certain situations. Several previous attempts have been made to correct these discrepancies (see, for example Adams et al, [2]). In this paper we restrict ourselves to regular Cartesian geometry, and introduce Discontinuity Factors [3] to avoid these inconsistencies. By doing so, we correctly reproduce the transport theory currents in a diffusion theory-like framework. This results in a fully consistent DSA, which we shall call the eDSA, where "e" stands for equivalence theory. In many respects, the method is similar to a Coarse Mesh Finite Difference (CMFD) acceleration method (see, for example, Masiello [4] and Hong, Kim & Song [5] and references therein), but with the coarse mesh exactly equivalent to the fine mesh. The major difference is the use of the eDSA technique

to accelerate both the within-group flux solution (inner iterations) and also the group-group fission source and scattering iterations (outer iterations).

Discontinuity Factors (DF) are more usually encountered in the context of the spatial homogenisation of flux weighted constants from fine mesh lattice physics cell or assembly calculations for use in coarser mesh "nodal" 3D whole core solvers. The equations developed are known as the equivalence relations, and enable the calculation of the correct reaction rates and interfacial currents on the coarse mesh basis; in this paper we use the same relations, but will not apply spatial homogenisation, ie the same fine mesh is used both for the transport theory solution and the diffusion theory like acceleration solution. As noted above, when homogenisation is applied, this method is generally known as Coarse Mesh Finite Difference acceleration.

This paper will only consider the eDSA applied to the solution of the multigroup S_N finite difference discrete ordinates transport equation in rectilinear geometry. Isotropic scattering will be assumed for simplicity, although Rolls-Royce have a code working with anisotropic scatter. Section 4 contains some thoughts about how the eDSA might be applied to the acceleration of other transport theory methods, such as the method of characteristics.

The success of the acceleration technique is predicated on the availability of a fast and reliable solver for the diffusion-theory-like equivalence relations. In this work we use a straightforward finite difference multigrid solver. This has the major advantage that this solution technique solves the relations on all spatial scales at once. The success of the acceleration technique depends crucially on this behavior.

Un-accelerated transport theory solution techniques are generally good at the prediction of local fluxes and local interfacial currents, but poor at propagating longer range variations across the problem. This is particularly true of the S_N method considered here. A minimal number of transport theory solver sweeps will usually be sufficient to obtain a good approximation to the local transport theory interfacial currents, enabling the calculation of relatively accurate local discontinuity factors. The use of a multigrid technique to solve the eDSA equations provides the mechanism by which long range interactions are quickly propagated across the whole problem, thus providing the necessary overall acceleration of the transport theory solution.

Two levels of acceleration are proposed in a k_{eff} solution (as usually employed in reactor physics lattice calculations):

a) Acceleration of the transport theory inner iteration sweeps – ie acceleration of the calculation of the within-group flux distribution. This is achieved by solution of the eDSA equations by the multigrid method and subsequent scaling of the mesh-wise angular fluxes by the ratio of the post-eDSA scalar flux to the pre-eDSA scalar flux. For mesh boundary angular fluxes, the ratio used is that appropriate to the mesh for which the angular flux is outgoing.

b) Acceleration of the estimation of the fission source and k_{eff}, ie acceleration of the outer iterations of the power method, and also acceleration of any additional group-group

scattering iterations. In this manner, the eDSA acceleration technique may also be applied to multigroup fixed external source problems. This involves performing one or more inner iterations for each energy group, and then preservation of the group-wise discontinuity factors. The eDSA relations are then solved for the fission source and k_{eff}, with possibly additional scattering iterations, without performing additional transport theory sweeps within these inner iterations. This provides an improved estimate of fission source and k_{eff} (and scalar flux) for use in the next set of transport theory inner iterations. An improved estimate of angular flux is obtained as above by scaling by the ratio of the post-eDSA to pre-eDSA scalar flux in each mesh. This use of the the eDSA relations is where the method described here most closely resembles a CMFD method.

Experience has shown that both techniques provide an improvement in convergence, but that acceleration of the outer iterations is especially advantageous. We will illustrate this in Section 3 by reference to the C5G7 OECD/NEA benchmark problem [6].

Rolls-Royce have been using this eDSA acceleration technique within the 2D transport theory solver MDLTRAN incorporated in the bespoke lattice physics code RAPID since the early 1990's. MDLTRAN solves the S_N discrete ordinates equation in multi-groups (typically ten) on a rectilinear mesh (problem sizes typically 250*250 meshes) using a linear discontinuous spatial transport theory discretisation. RAPID also includes generation of multi-group cross-sections (including resonance self shielding correction), the coupled neutron-gamma flux solution, mesh-wise depletion of fuel and absorber number densities, the generation of homogenised cross-sections for use in our bespoke coarse mesh whole core code, and fine mesh flux synthesis factors and for 3D fine mesh reconstruction.

Rolls-Royce are currently extending the MDLTRAN solver into 3D, parallelising the code by energy group and by z-band using MPI. The results given in Section 3 were actually produced using a prototype version of this code parallelised by energy group.

2. THEORY

2.1. S_N Discrete Ordinates Transport Equation

The multi-group steady state Boltzmann transport equation in rectilinear geometry with isotropic scatter is:

$$\Omega . \nabla \psi^g(x,y,z,\Omega) \; + \; \Sigma^g{}_t(x,y,z)\psi^g(x,y,z,\Omega) \; = \; Q^g{}_s(x,y,z) \; + \; Q^g{}_f(x,y,z) \quad (1)$$

where $\psi^g(x,y,z,\Omega)$ is the angular flux in energy group g, and

$$Q^g{}_s(x,y,z) \; = \; \sum_{g'} \Sigma_s^{g' \Rightarrow g}(x,y,z) \;\; \phi^{g'}(x,y,z) \quad (2a)$$

$$Q^g{}_f(x,y,z) \; = \; \frac{\chi^g}{k_{eff}} \;\; \sum_{g'} \nu \Sigma_f^{g'}(x,y,z) \;\; \phi^{g'}(x,y,z) \quad (2b)$$

are the scatter and fission sources respectively. $\phi^g(x,y,z)$ is the scalar flux:

$$\phi^g(x,y,z) = \frac{1}{4\pi} \int \psi^g(x,y,z,\underline{\Omega}) \, d\Omega \tag{3}$$

Making the usual S_N discrete ordinates approximation, $\phi^g(x,y,z) = \sum_m W_m \psi^g_m(x,y,z)$ where W_m is the weight associated with each solid angle Ω_m in direction *m*, we have:

$$\Omega . \nabla \psi^g_m(x,y,z) + \Sigma^g{}_t(x,y,z)\psi^g_m(x,y,z) = Q^g{}_s(x,y,z) + Q^g{}_f(x,y,z) \tag{4}$$

Restricting ourselves to a rectilinear mesh (with constant materials properties within each mesh volume), integrating over mesh volumes and making use of Gauss's theorem $\int dV \nabla f(x,y,z) = \oint dS \, f(x,y,z)$ (and dividing throughout by the mesh volume), we obtain:

$$\mu_m \frac{(\psi^g_{m\ i+1/2,j,k} - \psi^g_{m\ i-1/2,j,k})}{\Delta x_i} + \eta_m \frac{(\psi^g_{m\ i,j+1/2,k} - \psi^g_{m\ i,j-1/2,k})}{\Delta y_j} + \xi_m \frac{(\psi^g_{m\ i,j,k+1/2} - \psi^g_{m\ i,j,k-1/2})}{\Delta z_k} + \Sigma^g_{t\ i,j,k} \psi^g_{m\ i,j,k} = Q^g_{s\ i,j,k} + Q^g_{f\ i,j,k} \tag{5}$$

where μ_m, η_m and ξ_m are the direction cosines of Ω_m along the *x*, *y* and *z* axis respectively, $\psi^g_{m\ i-1/2,j,k}$ etc are the mesh face average angular fluxes in direction Ω_m, $\Sigma^g_{t\ i,j,k}$ is the mesh average total cross-section (usually replaced by the transport cross-section in the isotropic scatter approximation), $\psi^g_{m\ i,j,k}$ is the mesh average angular flux, Δx_i, Δy_j, Δz_k are the *x*, *y* and *z* dimensions of mesh *(i,j,k)*, and $Q^g_{s\ i,j,k}$ and $Q^g_{f\ i,j,k}$ are the scatter and fission source terms respectively.

Summing over angle (with appropriate weights), we obtain:

$$J^g_{i-1/2,j,k} + J^g_{i+1/2,j,k} + J^g_{i,j-1/2,k} + J^g_{i,j+1/2,k} + J^g_{i,j,k-1/2} + J^g_{i,j,k+1/2} + \Sigma^g_{t\ i,j,k} \phi^g_{i,j,k} = Q^g_{s\ i,j,k} + Q^g_{f\ i,j,k} \tag{6}$$

where $J^g_{i-1/2,j,k}$ is the average interfacial current (in the positive x direction) at the left hand face of mesh *(i,j,k)* (a negative value of current indicates a nett outflow from this face), $J^g_{i+1/2,j,k}$ is the current at the right face of mesh *(i,j,k)* (a positive current on this face indicates a nett outflow from mesh *(i,j,k)),* with similar terms for the *y* and *z* interfacial currents. $\phi^g_{i,j,k}$ is the mesh average scalar flux. In terms of angular fluxes, the interfacial currents are given by:

$$
\begin{aligned}
J^g_{i-1/2,j,k} &= \sum_m W_m \ \mu_m \psi^g_{m\ i-1/2,j,k} & J^g_{i+1/2,j,k} &= \sum_m W_m \ \mu_m \psi^g_{m\ i+1/2,j,k} \\
J^g_{i,j-1/2,k} &= \sum_m W_m \ \eta_m \psi^g_{m\ i,j-1/2,k} & J^g_{i,j+1/2,k} &= \sum_m W_m \ \eta_m \psi^g_{m\ i,j+1/2,k} \\
J^g_{i,j,k-1/2} &= \sum_m W_m \ \xi_m \psi^g_{m\ i,j,k-1/2} & J^g_{i,j,k-1/2} &= \sum_m W_m \ \xi_m \psi^g_{m\ i,j,k+1/2}
\end{aligned}
\tag{7}
$$

The face (average) angular fluxes are obtained during the transport theory solution using a linear difference (or higher order) approximation, for example, at the simplest, the diamond difference approximation is given by :

$$
\begin{aligned}
2\psi^g_{m\ i,j,k} &= \psi^g_{m\ i-1/2,j,k} + \psi^g_{m\ i+1/2,j,k} \\
2\psi^g_{m\ i,j,k} &= \psi^g_{m\ i,j-1/2,k} + \psi^g_{m\ i,j+1/2,k} \\
2\psi^g_{m\ i,j,k} &= \psi^g_{m\ i,j,k-1/2} + \psi^g_{m\ i,j,k+1/2}
\end{aligned}
\tag{8}
$$

The transport theory solution in its simplest form is performed by substituting the diamond difference approximation (8) into the discretised form of the transport equation (5), eliminating the unknown boundary angular fluxes, and sweeping across the problem from the outer boundaries, following the direction of Ω_m . For example, if Ω_m is in the positive *x, y, z* octant, then, in mesh (*i,j,k*), the boundary angular fluxes at the mesh faces at *i-1/2, j-1/2, k-1/2* are known, and putting the difference approximations $\psi^g_{m\ i+1/2,j,k} = 2\psi^g_{m\ i,j,k} - \psi^g_{m\ i-1/2,j,k}$ etc into (5) we obtain an expression for $\psi^g_{m\ i,j,k}$ purely in terms of known quantities. Thus, given boundary angular fluxes on three of the six faces of each mesh, we can estimate the mesh average flux, and then use the diamond difference relations (8) to estimate the other three unknown boundary fluxes. We can then move to the next mesh along in *x, y* or *z*. Application of external boundary conditions is necessary to make the problem complete.

2.2. Diffusion Synthetic Acceleration

In the standard DSA, the usual diffusion theory approximation is made for the boundary current, ie, in finite difference terms we have:

$$
\begin{aligned}
J^g_{i-1/2,j,k} &= -D^g(x,y,z)\nabla\phi^g(x,y,z) \\
&= \frac{-\tilde{D}^g_{i,j,k}(\phi^g_{i,j,k}-\phi^g_{i-1/2,j,k})}{\Delta x_i/2} \\
&= \frac{-\tilde{D}^g_{i-1,j,k}(\phi^g_{i-1/2,j,k}-\phi^g_{i-1,j,k})}{\Delta x_{i-1}/2} \\
&= \frac{-2\tilde{D}^g_{i,j,k}\tilde{D}^g_{i-1,j,k}(\phi^g_{i,j,k} - \phi^g_{i-1,j,k})}{\Delta x_{i-1}\tilde{D}^g_{i,j,k} + \Delta x_i \tilde{D}^g_{i-1,j,k}}
\end{aligned}
\tag{9}
$$

where $\tilde{D}^g_{i,j,k}$ is the diffusion coefficient in mesh *i,j,k*, conventionally set to one third of the inverse transport cross-section $\tilde{D}^g_{i,j,k}=1/(3\Sigma_{tr\ i,j,k})$.

The standard DSA requires the definition of the mesh wise diffusion coefficient such that the transport theory currents are reproduced by relations of type (9) correctly for all six directions. Unfortunately, in practice, this proves to be impossible without the introduction of directionally dependent diffusion coefficients. Several attempts have been made to improve on this approximation in the past (see, for example, [2]), but these have not been entirely successful.

2.3. Equivalence Theory

In equivalence theory we relax the requirement for continuity of scalar fluxes on the mesh boundaries, and define discontinuity factors [3]:

$$f^{g\ x+}_{i,j,k} \equiv \frac{\phi^{g}_{i+1/2,j,k}}{\phi^{g\ x+}_{i,j,k}} \quad , \quad f^{g\ x-}_{i,j,k} \equiv \frac{\phi^{g}_{i-1/2,j,k}}{\phi^{g\ x-}_{i,j,k}} \tag{10}$$

where $\phi^{g}_{i+1/2,j,k}$ and $\phi^{g}_{i-1/2,j,k}$ are the true transport theory prediction of face average boundary scalar flux, and $\phi^{g\ x+}_{i,j,k}$ and $\phi^{g\ x-}_{i,j,k}$ are the mesh boundary fluxes necessary to produce the correct transport theory currents in the diffusion theory like framework. Using finite difference diffusion theory (the relations would be more complicated if a higher order nodal solution were to be employed to solve the diffusion theory like relations) we have:

$$\phi^{g\ x+}_{i,j,k} = \phi^{g}_{i,j,k} - \frac{J^{g}_{i+1/2,j,k}\Delta x_i}{2\ \tilde{D}^{g}_{i,j,k}} \quad , \quad \phi^{g\ x-}_{i,j,k} = \phi^{g}_{i,j,k} + \frac{J^{g}_{i-1/2,j,k}\Delta x_i}{2\ \tilde{D}^{g}_{i,j,k}} \tag{11}$$

Eliminating $\phi^{g\ x+}_{i,j,k}$ and $\phi^{g\ x-}_{i,j,k}$ we obtain:

$$J^{g}_{i-1/2,j,k} = \frac{-2\,\tilde{D}^{g}_{i,j,k}\tilde{D}^{g}_{i-1,j,k}\left(f^{g\ x-}_{i,j,k}\ \phi^{g}_{i,j,k} - f^{g\ x+}_{i-1,j,k}\phi^{g}_{i-1,j,k}\right)}{\Delta x_{i-1} f^{g\ x+}_{i-1,j,k}\tilde{D}^{g}_{i,j,k} + \Delta x_i f^{g\ x-}_{i,j,k}\ \tilde{D}^{g}_{i-1,j,k}} \tag{12}$$

Comparing equation (12) with (9) we see that the standard diffusion coefficient has been replaced by $\frac{\tilde{D}^{g}_{i,j,k}}{f^{g\ x\pm}_{i,j,k}}$, ie we have directionally dependent diffusion coefficients, but that, in the numerator, the fluxes are also multiplied by the discontinuity factors. Thus the equivalence theory has introduced more than directionally dependent diffusion coefficients. Similar expressions hold in *y* and *z*. Note that in void or low interaction regions, where $\Sigma_{tr\ i,j,k}$ is near zero, within the eDSA model, the diffusion coefficient can be set to an arbitrary large value such that multiplication by infinity or near infinity is avoided; the definition of the discontinuity factor will still correctly reproduce the interfacial current in such situations.

Thus, following a series of transport theory sweeps, approximate mesh interfacial currents are obtained, and approximate discontinuity factors may be calculated using equations (10) and (11).

The equivalence theory like relations are thus (multiplying both sides of the the transport equation by the mesh volume):

$$\begin{aligned} -D^g_{x\ i-1/2,j,k}\ f^{g\ x+}_{i-1,j,k}\ \phi^g_{i-1,j,k} - D^g_{x\ i+1/2,j,k}\ f^{g\ x-}_{i+1,j,k}\ \phi^g_{i+1,j,k} \\ -D^g_{y\ i,j-1/2,k}\ f^{g\ y+}_{i,j-1,k}\ \phi^g_{i,j-1,k} - D^g_{y\ i,j+1/2,k}\ f^{g\ y-}_{i,j+1,k}\ \phi^g_{i+1,j,k} \\ -D^g_{z\ i,j,k-1/2}\ f^{g\ z+}_{i,j,k-1}\ \phi^g_{i,j,k-1} - D^g_{z\ i,j,k+1/2}\ f^{g\ z-}_{i,j,k+1}\ \phi^g_{i,j,k+1} \\ +A^g_{t\ i,j,k}\ \phi^g_{i,j,k} = V_{i,j,k}Q^g_{s\ i,j,k} + V_{i,j,k}Q^g_{f\ i,j,k} \end{aligned} \tag{13}$$

where

$$D^g_{x\ i-1/2,j,k} \equiv \frac{-2\,\tilde{D}^g_{i,j,k}\tilde{D}^g_{i-1,j,k}\Delta y_j \Delta z_k}{\Delta x_{i-1} f^{g\ x+}_{i-1,j,k}\tilde{D}^g_{i,j,k} + \Delta x_i f^{g\ x-}_{i,j,k}\ \tilde{D}^g_{i-1,j,k}} \tag{14}$$

with similar terms in *y* and *z*, and:

$$\begin{aligned} A^g_{t\ i,j,k} \equiv D^g_{x\ i-1/2,j,k}\ f^{g\ x-}_{i,j,k} + D^g_{x\ i+1/2,j,k}\ f^{g\ x+}_{i,j,k} + \\ D^g_{y\ i,j-1/2,k}\ f^{g\ y+}_{i,j,k} + D^g_{y\ i,j+1/2,k}\ f^{g\ y-}_{i,j,k} + \\ D^g_{z\ i,j,k-1/2}\ f^{g\ z+}_{i,j,k} + D^g_{z\ i,j,k+1/2}\ f^{g\ z-}_{i,j,k} + \\ V_{i,j,k}\Sigma^g_{t\ i,j,k} \end{aligned} \tag{15}$$

Note that the use of non-return (or vacuum) boundary conditions in transport theory requires a special definition of discontinuity factor on such boundaries. This is set by the value of scalar flux assumed within the diffusion theory like solution; at present we use $\phi^g_{Nx+1,j,k} = -\phi^g_{Nx,j,k}$ which leads to $\phi^{g\ x+}_{Nx+1/2,j,k} = 0$, ie a zero flux boundary condition within the diffusion theory solution method.

In practice the self-scatter contribution is subtracted from both sides of equation (13) (this makes the solution more stable), thus giving:

$$\begin{aligned} -D^g_{x\ i-1/2,j,k}\ f^{g\ x+}_{i-1,j,k}\ \phi^g_{i-1,j,k} - D^g_{x\ i+1/2,j,k}\ f^{g\ x-}_{i+1,j,k}\ \phi^g_{i+1,j,k} \\ -D^g_{y\ i,j-1/2,k}\ f^{g\ y+}_{i,j-1,k}\ \phi^g_{i,j-1,k} - D^g_{y\ i,j+1/2,k}\ f^{g\ y-}_{i,j+1,k}\ \phi^g_{i+1,j,k} \\ -D^g_{z\ i,j,k-1/2}\ f^{g\ z+}_{i,j,k-1}\ \phi^g_{i,j,k-1} - D^g_{z\ i,j,k+1/2}\ f^{g\ z-}_{i,j,k+1}\ \phi^g_{i,j,k+1} \\ +A^g_{r\ i,j,k}\ \phi^g_{i,j,k} = V_{i,j,k}Q^g_{r\ i,j,k} + V_{i,j,k}Q^g_{f\ i,j,k} \end{aligned} \tag{16}$$

with

$$\begin{aligned} A^g_{r\ i,j,k} \equiv D^g_{x\ i-1/2,j,k}\ f^{g\ x-}_{i,j,k} + D^g_{x\ i+1/2,j,k}\ f^{g\ x+}_{i,j,k} + \\ D^g_{y\ i,j-1/2,k}\ f^{g\ y+}_{i,j,k} + D^g_{y\ i,j+1/2,k}\ f^{g\ y-}_{i,j,k} + \\ D^g_{z\ i,j,k-1/2}\ f^{g\ z+}_{i,j,k} + D^g_{z\ i,j,k+1/2}\ f^{g\ z-}_{i,j,k} + \\ V_{i,j,k}\Sigma^g_{r\ i,j,k} \end{aligned} \tag{17}$$

and

$$Q^{g}{}_{r}(x,y,z) = \sum_{g' \neq g} \Sigma_{s}^{g' \Rightarrow g}(x,y,z)\ \phi^{g'}(x,y,z) \tag{18}$$

where $\Sigma^{g}_{r\ i,j,k} = \Sigma^{g}_{t\ i,j,k} - \Sigma_{s}^{g \Rightarrow g}(x,y,z)$ is the removal cross-section.

2.4. Multigrid Method

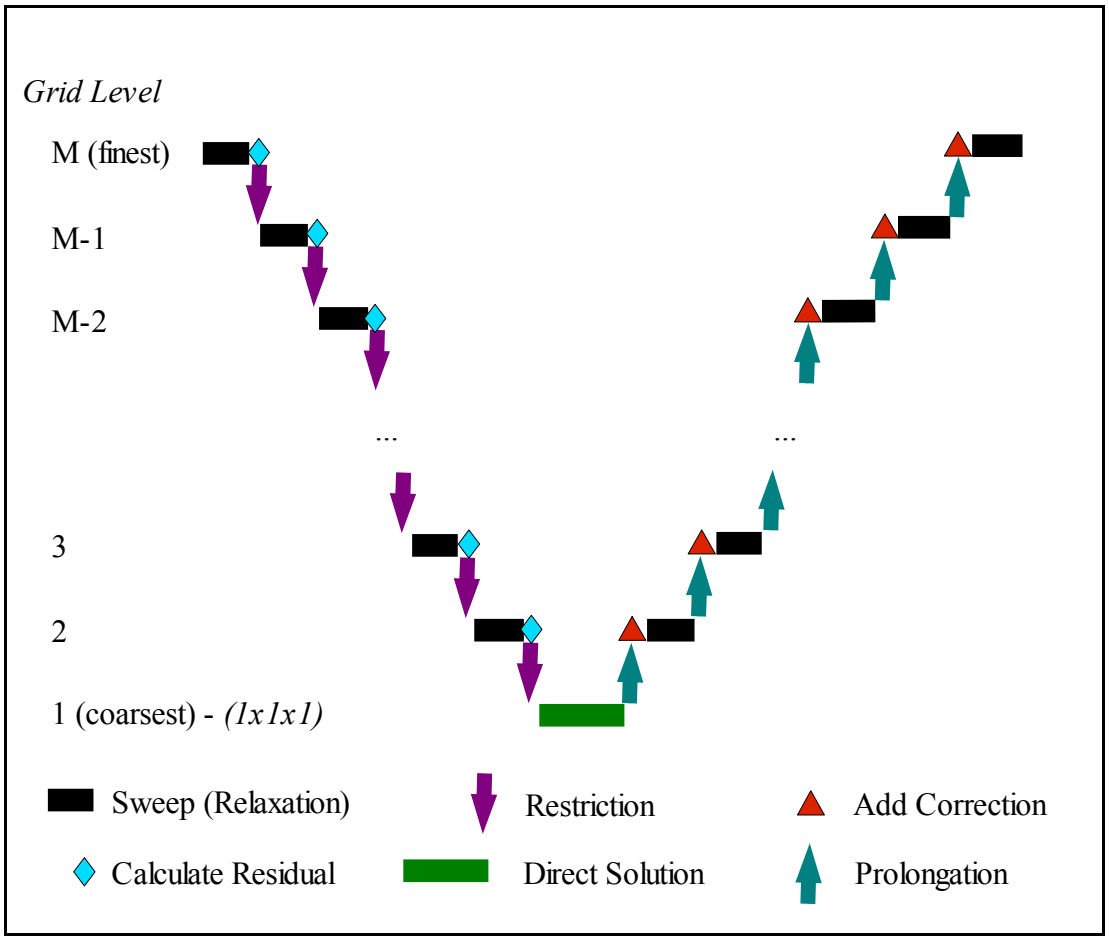

Figure 1. Multigrid Method

The equivalence theory relations have the same structure as the diffusion theory relations and may be solved using the same techniques. The most efficient technique developed to date is probably the multigrid method. Working within an energy group, the diffusion (or equivalence theory) relations are solved (a sweep is performed across the problem – in this context this is known as a *relaxation*) with the current values of fission and scatter sources. Following the sweep, mesh wise *residuals* are calculated (ie the differences between the *lhs* and *rhs* of the equivalence relations). These residuals are then *restricted* onto a coarser grid structure, and the

same sweep across the problem is performed (*relaxation*) on this coarser grid structure, using the restricted residual as the source term on the *rhs* of the coarser mesh equations, solving for a *correction* to be applied on the finer mesh grid when *prolonged* back from the coarse grid to the finer grid. The residual from this sweep is itself *restricted* to an even coarser grid to act as the source for a sweep across the problem on this even coarser grid. The method is illustrated in Figure 1. Ultimately a solution is required on a *(1x1x1)* grid, for which a direct solution is possible. The coarse sweep solution parameters are then *prolonged* onto the finer grids as finer grid corrections to improve the overall estimate of the sweep parameter on that grid. Further sweeps (relaxations) are then performed on that grid level before prolonging the grid sweep solution parameter to the next finer grid level as the correction on that level. Ultimately, the finest correction is added to the fine mesh flux to produce a better estimate of flux, incorporating improvements made at all coarser (ie longer) length scales. In Cartesian geometry the *restriction* is a simple volume weighting operation, whereas the *prolongation* is an interpolation procedure. Care must be taken with any "odd" meshes when defining coarser grid structures making sure that similar mesh dimensions are retained across the whole problem on all grids. Note that boundary conditions need to be applied within the sweep procedure at all grid levels.

When convergence is achieved on the finest grid level, then the residual is zero, leading to zero source on all coarser grid levels, and zero corrections on every grid level. Thus any approximations made during *restriction* and *prolongation* are unimportant once final convergence is achieved.

We take advantage of this behavior of the multigrid method in the solution of the equivalence relations by not defining or using discontinuity factors on any of the coarser grid levels, ie the equations solved here just make use of the mesh dimensions and the volume weighted diffusion coefficient and total (removal) cross-section. This provides a considerable computing saving as the coarser grid factors $D^g_{x\ i-1/2,j,k}$ etc and $A^g_{r\ i,j,k}$ need only be defined once at the start of the problem, and stored for later use. The finest grid factors must be updated every time the discontinuity factors are updated (ie after every transport theory sweep).

2.5. eDSA Method

The iteration strategy for the full eDSA method (as applied to both inner and outer (power method) iterations) is shown in Figure 2 below. This shows that, compared to the un-accelerated solution, the extra computational effort is spent in calculating the discontinuity factors (once every transport theory sweep), and in the solution of the eDSA relations using the multigrid solver. This has particular importance for the solution of problems with high order quadrature – the additional cost of the eDSA acceleration does not increase with S_N order (there is a minimal increase in cost when calculating the interfacial currents and in performing the scaling of angular fluxes), and hence the eDSA technique becomes proportionally more efficient as the S_N order increases. This will be shown for the C5G7 test problem in Section 3 below.

Note that Figure 2 shows either a sweep through the energy groups (it is usual to start from the highest energy group and work down in energy) or a scattering iteration; the former is more appropriate where data from all energy groups is stored on the same processor, whereas the scattering iteration is more appropriate for a method parallelised by energy group.

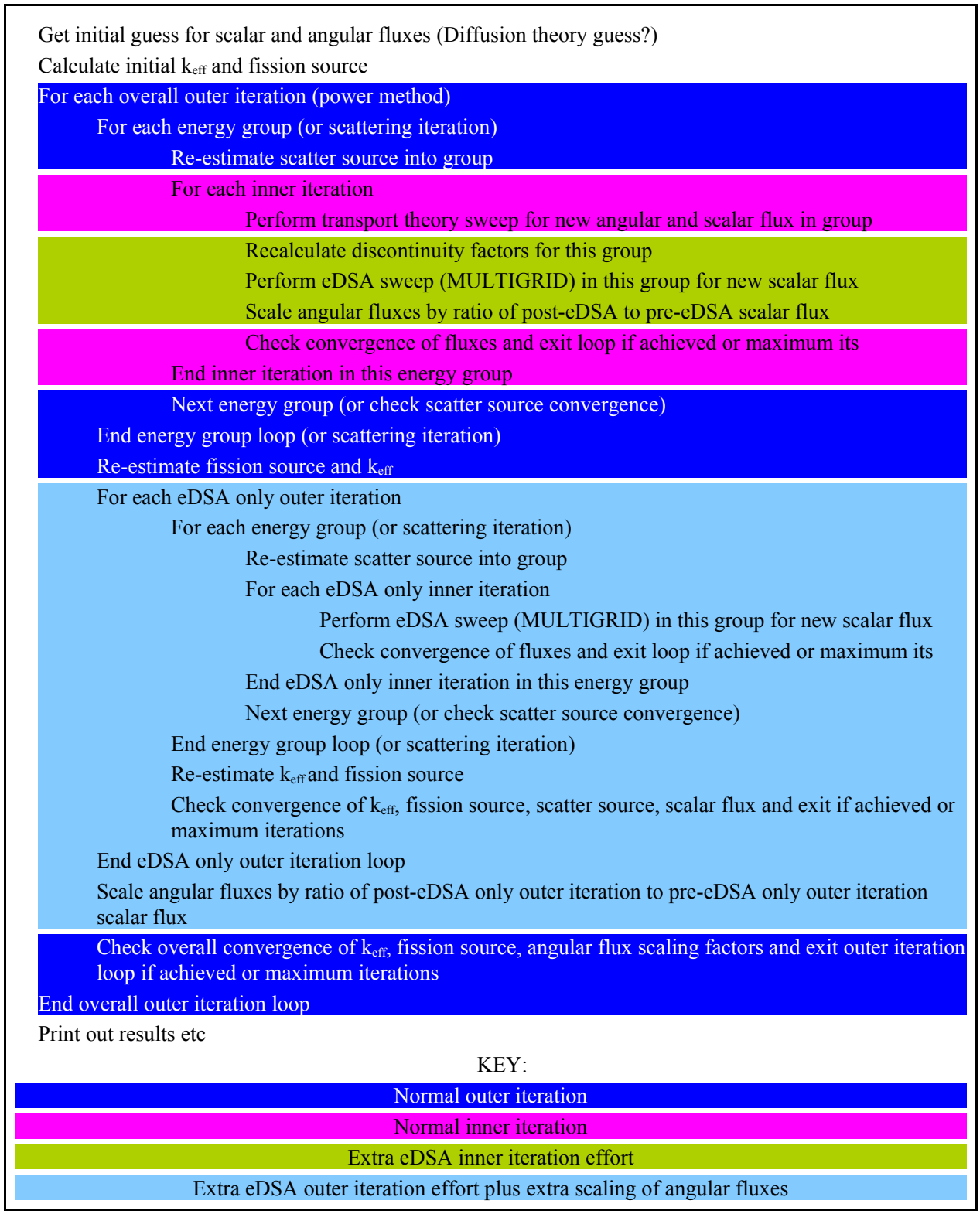

Figure 2. eDSA Iteration Strategy

For problems without a fission source, the eDSA can still be applied to accelerate the convergence of the group-group scattering source term, following the sequence of Figure 2, but leaving out the steps where k_{eff} and the fission source are re-estimated. The method is thus equally applicable to problems where the fission source is replaced by a fixed external source. Note that conventional fission source acceleration techniques, such as Tchebychev acceleration, or Successive Over Relaxation, can still be applied if required.

Finally note that the eDSA technique can also be successfully applied to the solution of the adjoint transport equation.

3. TEST CASES

We will illustrate the performance of the eDSA scheme by reference to the OECD NEA 2D C5G7 benchmark problem [6]. This was originally devised to test the accuracy of various transport theory codes to correctly reproduce a neutron flux solution for a lattice array of fuel pins without spatial homogenisation. It was chosen in this context simply as a well known multi-group problem for which a known solution is published. In this paper we shall not consider the effect of modelling round pins on a Cartesian lattice, or the effects of different S_N orders on the accuracy of the solution. Instead we shall concentrate on the properties of the eDSA acceleration technique.

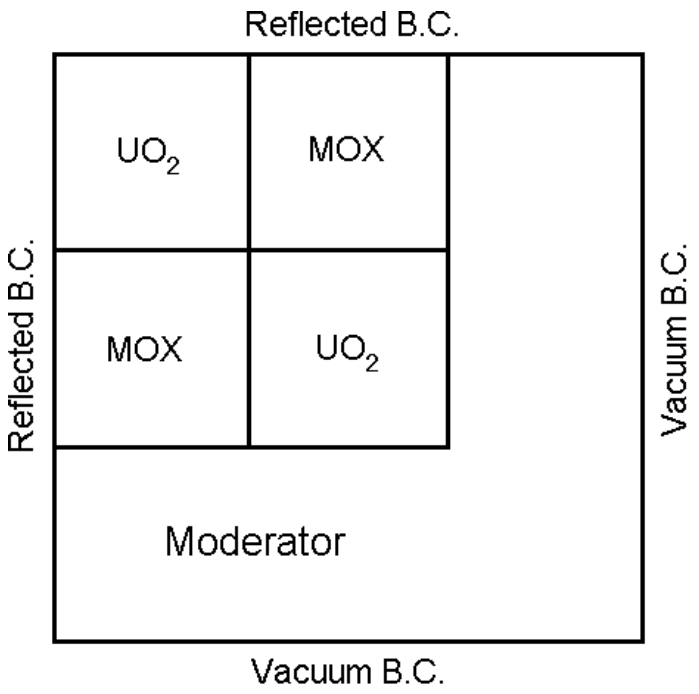

Figure 3. G5G7 2D Benchmark Core Configuration

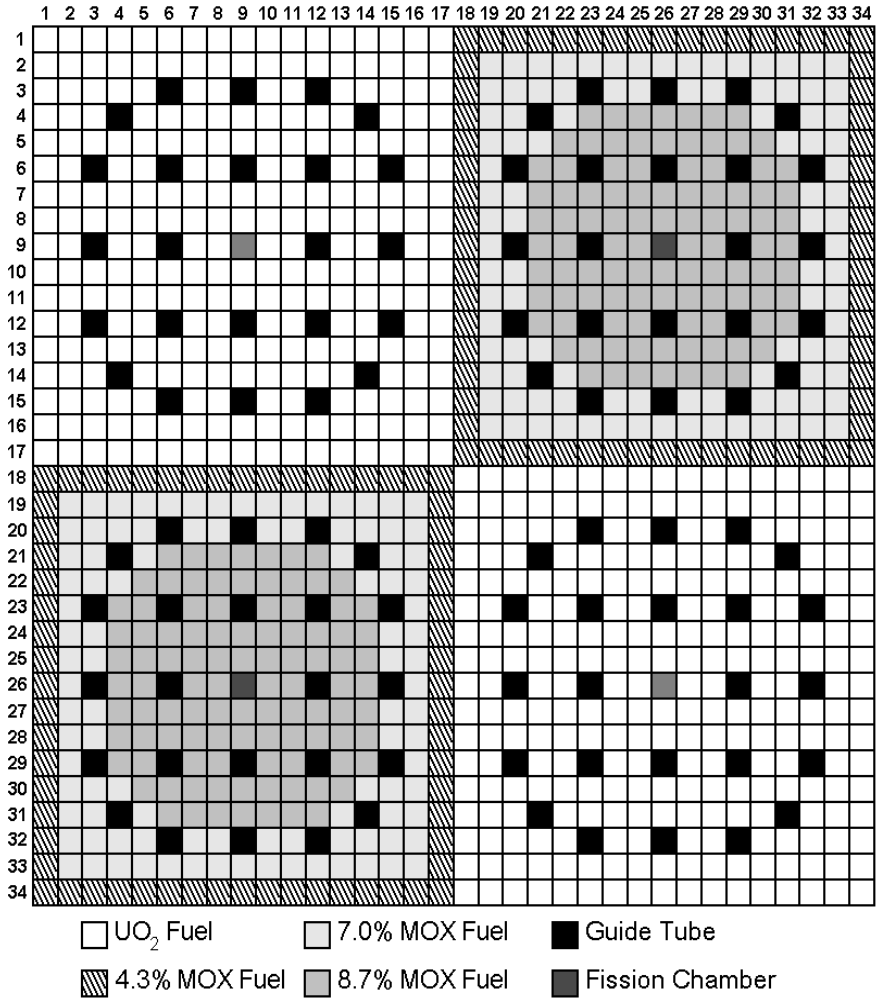

Figure 4. C5G7 Lattice Arrangement

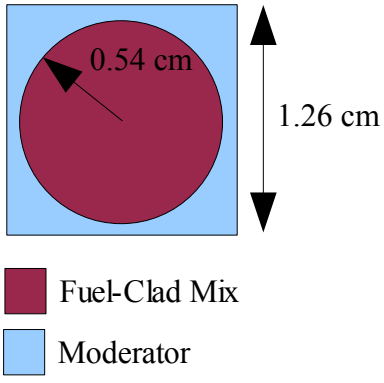

Figure 5. C5G7 Fuel Pin Arrangement

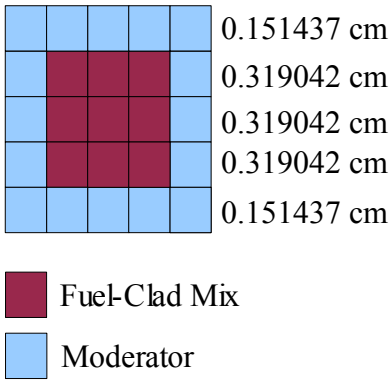

Figure 6. Equal Area Fuel Pin Model

The C5G7 test problem consists of four 17x17 fuel pin assemblies (sized at 21.42cm) and a region of side reflector water (also 21.42cm thick) as shown in Figure 3 below. Each assembly has a number of control rod guide tubes and a central fission chamber as shown in Figure 4. Two of the assemblies contain only UO_2 fuel, whereas the other two assemblies contain MOX fuel with fuel pins containing varying levels of U/Pu mixes. The fuel pins themselves are modelled as a cylindrical fuel/clad mix (radius 0.54cm) surrounded by moderator, as shown in Figure 5. The pin pitch is 1.26 cm. The benchmark specification contains 7 group cross-section data for each material, and gives a reference MCNP fuel pin fission rate distribution and k_{eff}.

The benchmark was modelled using a simple 5x5 rectilinear mesh per fuel pin, with mesh spacings chosen to give an equal area approximation, as shown in Figure 6 above, ie the cross-sectional area of the square pin matched that of the real cylindrical fuel pin. In practice this turns out to be a reasonable approximation, although the accuracy of the results will not be discussed here. The side reflector was modelled using 10x0.4284 meshes closest to the fuel and an outer 20x0.8568 cm meshes leading to a problem size of 200x200 meshes.

The neutron flux and k_{eff} were obtained using the RR MDLTRAN solver modified to switch off the eDSA acceleration during inner and outer iterations. This version of the code had also been parallelised by energy group, and thus included the option to perform extra scattering iterations during the outer iterations – all the cases that follow used just one scattering iteration surrounding the normal transport theory inner iteration sweeps, but used a maximum of seven scattering iterations around the extra eDSA inner iteration sweeps performed within the extra eDSA outer iteration. These additional scattering iterations were terminated if the relative change in scattering source was sufficiently small. All problems started with the same diffusion theory flux guess. A full set of solutions with different convergence parameters was performed using both S_4 and S_{16} quadrature. The choices are shown in Table 1 below, along with the number of outer iterations taken to convergence (relative change in fission source, scatter source, scalar flux and post-eDSA to pre-eDSA scalar flux scaling factor divergence from unity all < 0.0001, relative change in k_{eff} < 0.000001).

Table 1. Outer Iteration Convergence

Maximum Number of Inner Iterations per Outer Iteration	Outer eDSA applied	Inner eDSA applied	Number of Outer Iterations to Convergence (S_4)	Number of Outer Iterations to Convergence (S_{16})
1	Yes	Yes	36	34
2	Yes	Yes	15	15
3	Yes	Yes	15	15
4	Yes	Yes	15	15
5	Yes	Yes	15	15
10	Yes	Yes	15	15
1	No	Yes	158	156
2	No	Yes	158	156
3	No	Yes	158	156
4	No	Yes	158	156
5	No	Yes	158	156
10	No	Yes	158	156
1	No	No	500	500
2	No	No	344	331
3	No	No	254	245
4	No	No	211	209
5	No	No	187	191
10	No	No	167	169

The fission source convergence vs outer iteration number with S_4 quadrature is shown in Figure 7. This shows that, with no eDSA acceleration, the number of outer iterations required for convergence decreases with the number of inner iterations per outer iteration. With acceleration, the number of iterations required for convergence and the rate of decrease of source convergence is almost independent of the number of inner iterations per outer iteration – indeed the lines lie on top of each other and can not be distinguished on this scale. The left-most (magenta) line is indicative of all the cases with both inner and outer acceleration, and the next line (cyan) represents all the cases with only inner iteration eDSA acceleration.

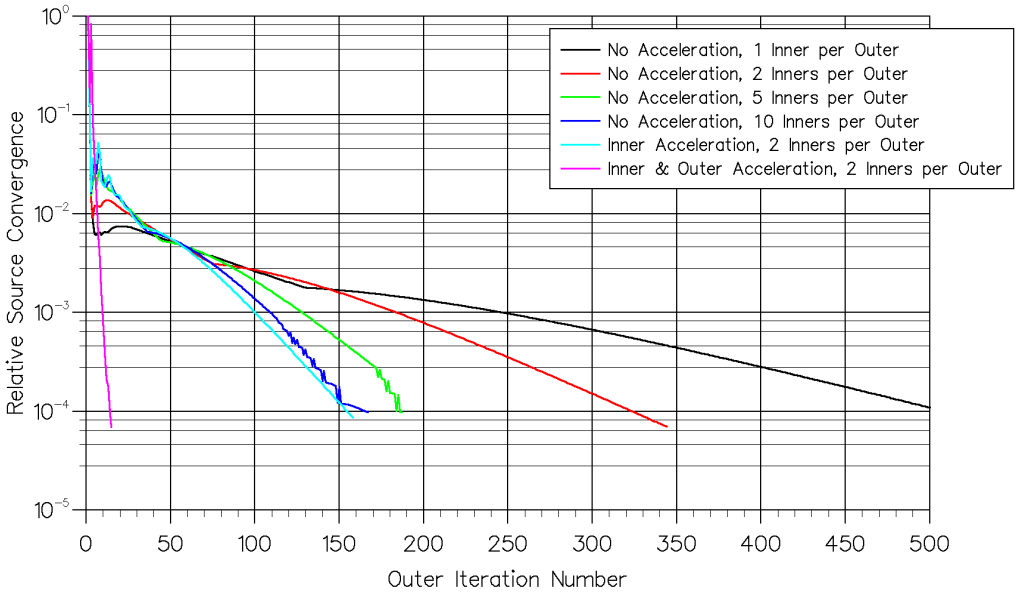

Figure 7. S_4 Fission Source Convergence vs Outer Iteration Number

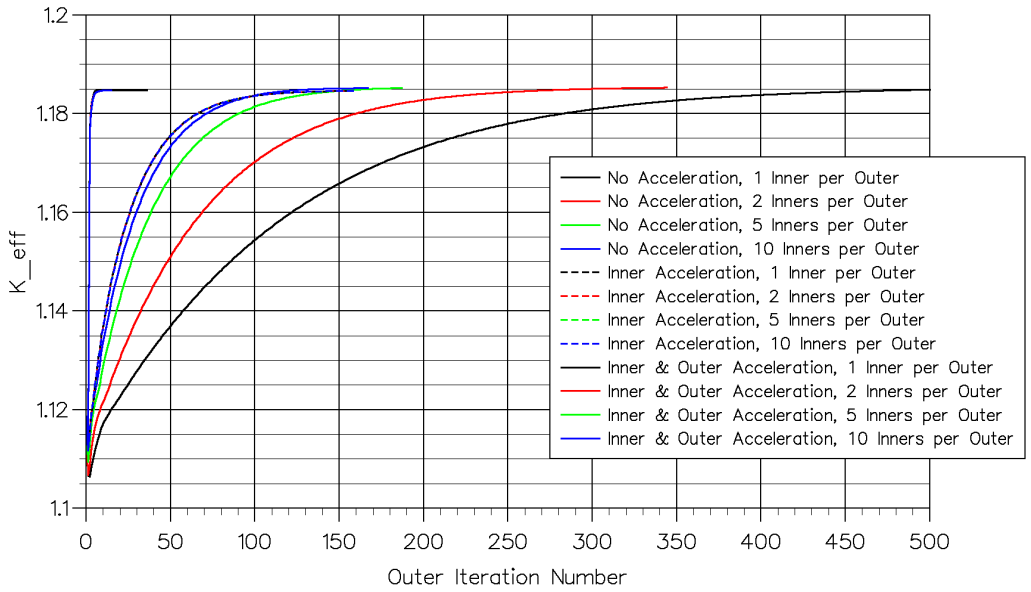

Figure 8. S_4 k_{eff} Convergence vs Outer Iteration Number

Figure 8 shows the k_{eff} convergence for S_4 quadrature against outer iteration number. The left-most line shows all the cases with both inner and outer iteration acceleration – these are not distinguishable from each other on this scale. The next line shows all the cases with only inner

iteration eDSA acceleration – they are also indistinguishable from each other. Only the cases with no eDSA acceleration show differences, the convergence is faster the more inner iterations are performed each outer iteration.

Table 1 shows that the number of iterations to convergence for S_{16} is very nearly the same as for S_4 quadrature. Indeed, the corresponding plots to Figures 7 and 8 for S_{16} are almost indistinguishable from the S_4 plots. For this reason they will not be reproduced here.

The same set of choices is the most effective for both quadratures, ie full inner and outer eDSA with a maximum of two normal inner iterations per outer iteration. This means that the most efficient method achieves the required convergence in only 15 outer iterations, ie only 30 transport theory sweeps, compared to the un-accelerated case where at least 500 transport theory sweeps are required (one inner per outer). Thus the fully accelerated eDSA provides at least a factor of ten decrease in the number of transport theory sweeps required for convergence.

Figures 9 and 10 show the relative compute times for the S_4 and S_{16} cases described in Table I. These times have been normalised to the 2 inner iterations per outer iteration fully accelerated cases (the cases that converged in the fastest time for each quadrature). These figures show that, although the eDSA always reduces the number of iterations to convergence, the extra cost of performing this on inner iterations alone may exceed the cost of additional transport theory sweeps. When both inner and outer iteration eDSA acceleration is applied however, the computational time is always smaller than when no acceleration is applied.

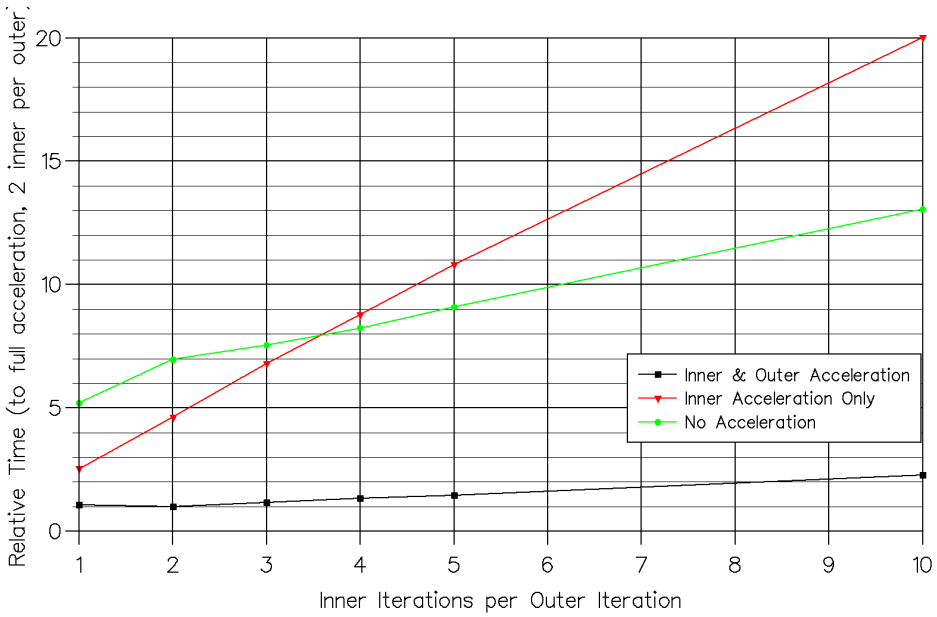

Figure 9. S_4 Relative Times to Convergence

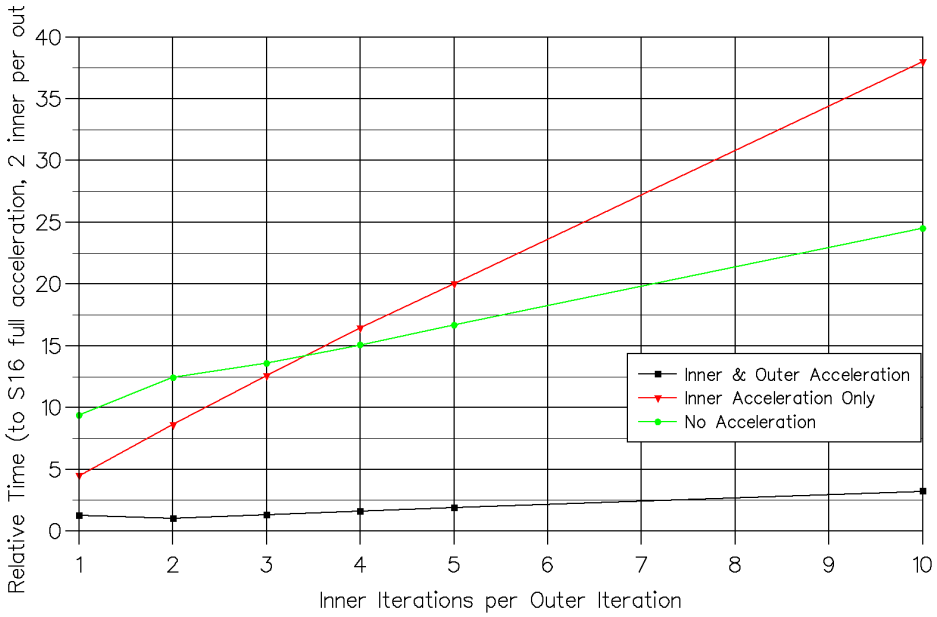

Figure 10. S_{16} Relative Times to Convergence

Figure 11 shows the relative fission source convergence rate for a number of different S_N quadratures using 2 inner iterations per outer iteration and full eDSA acceleration. Clearly the convergence rate is almost independent of quadrature order.

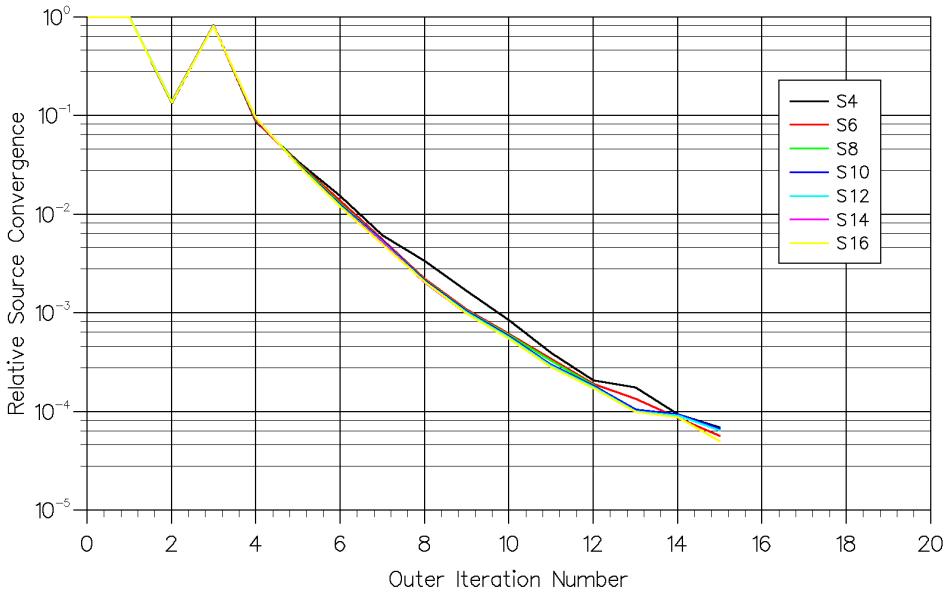

Figure 11. Fully Accelerated Source Convergence vs S_N order

Figure 12 shows the relative time taken to converge for these calculations. The time taken scales at less than order N. This is because most of the computing effort is spent in solving the eDSA relations rather than performing the computationally expensive transport theory sweeps. Thus the fully converged S_{16} solution is achieved in just over three times the computing time of the S_4 solution.

Figure 12. Fully Accelerated Relative Times to Convergence vs S_N order

4. POSSIBLE APPLICATION TO OTHER METHODS

As formulated here, the eDSA has been applied to the acceleration of the transport equation in Cartesian geometry with isotropic scattering. As mentioned earlier, RR have a code version capable of solving with anisotropic scatter, and with a higher order transport theory discretisation (without negative flux fix-up). This code version is used to solve for both neutron and gamma fluxes (with the gamma source term given by the neutron reaction rates). It also solves for adjoint fluxes, using the same eDSA acceleration technique. We are currently working on the development of a 3D whole core solver parallelising both by energy group and by spatial domain (bands in z). This code version will include some degree of adaptive mesh refinement to avoid negative angular fluxes where appropriate. It will also include fixed external sources.

Clearly the method as suggested here could be used as a pre-conditioner within a Krylov solver.

As it is closely related to CMFD acceleration techniques, the eDSA could also be applied to the solution of other transport theory solvers where a Cartesian grid can be overlaid on the base geometry. This might be particularly useful in the solution of a Method of Characteristics solver where it would be relatively easy to generate interfacial currents on such a grid, along with grid average cross-sections and scalar fluxes. This might also be possible within the framework of

unstructured finite element methods. Note, however, that convergence of the CMFD is not assured, especially for cases with very thick or very thin homogeneous regions in scattering dominated regimes (see Masiello [4] and references therein).

5. CONCLUSIONS

In this paper we have described the implementation of a consistent DSA-like acceleration technique for solution of the Boltzmann transport equation, and illustrated its advantages in the solution of the 2D C5G7 OECD NEA benchmark problem. We have shown how the eDSA provides benefit to the solution of the inner iteration of the transport theory solution, but provides most benefit to acceleration of the outer fission source iteration in a lattice physics code. We have also shown that by making use of this technique, the computational cost of higher order discrete ordinates solutions rises less rapidly than order N.

ACKNOWLEDGMENTS

The author wishes to thank all his colleagues at Rolls-Royce for their help, encouragement and assistance over the past twenty years.

REFERENCES

1. RE Alcouffe, “Diffusion synthetic acceleration methods for the diamond-differenced discrete ordinates equations”, *Nucl. Sci. Eng.*, **64**, pp.344-355 (1977).
2. ML Adams and WR Martin, *Nucl. Sci. Eng.*, **111**, pp.145-167 (1999).
3. AF Henry, *Nuclear Reactor Analysis,* MIT Press (1975).
4. E Masiello, “Analytical stability analysis of Coarse-Mesh Finite Difference method”, Proceedings of PHYSOR 2008, Interlaken, Switzerland, September 14-19, 2008.
5. Ser Gi Hong, Kang Seog Kim, Jae Seung Song, “On the Convergence of the Rebalance Methods for Transport Equation for Eigenvalue Problems”, Proceedings of PHYSOR 2008, Interlaken, Switzerland, September 14-19, 2008.
6. OECD NEA C5G7 “Benchmark on Deterministic Transport Theory Without Spatial Homogenisation”, NEA/NSC/DOC(2003)16.